Available online at www.sciencedirect.com

ScienceDirect

Procedia Chemistry 19 (2016) 113 – 118

Procedia Chemistry

5th International Conference on Recent Advances in Materials, Minerals and Environment (RAMM) & 2nd International Postgraduate Conference on Materials, Mineral and Polymer (MAMIP), 4-6 August 2015

Fabrication of tungsten oxide nanostructure by Sol-Gel method

Y. Chai, F.Y. Ha, F.K. Yam, Z. Hassan

Nano-Optoelectronic Research and Technology Laboratory, School of Physics, Universiti Sains Malaysia, Gelugor, Malaysia

Abstract

In this work, we present the effects of mixing sequence of sodium tungstate and nitric acid, as well as the aging duration on the formation of tungsten oxide by sol-gel method. Increase of the aging duration allows the formation of uniform platelet structure where no structure could be detected at 1 aging day while uniform platelet structure could be detected at 30 days. Hydrated tungsten oxide platelets of 1-1.θ ȝm could be formed by mixing sodium tungstate into nitric acid (sample labeled as W-A) which could be reduced significantly in size to 200-600 nm by changing the mixing sequence to drop nitric acid into sodium tungstate (sample labeled as A-W). Crystalline hydrated tungsten oxides were obtained for both samples where W-A sample shows better degree of crystallinity. Room temperature hydrogen gas sensing property was successfully detected by both samples where A-W sample demonstrates ~2.5 times higher sensor response to hydrogen gas compared to W-A sample.

Peer-review under responsibility of School of Materials and Mineral Resources Engineering, Universiti Sains Malaysia

Keywords: tungsten oxide; sol-gel; gas sensor

Nomenclature

WO_3	tungsten oxide	h	hour

* Corresponding author. Tel.: +60-46533599; fax: +60-46579150.
E-mail address: yqchai85@gmail.com

Peer-review under responsibility of School of Materials and Mineral Resources Engineering, Universiti Sains Malaysia
doi:10.1016/j.proche.2016.03.123

W-A	sample prepared by dropping Na_2WO_4 into HNO_3	min	minute
A-W	sample prepared by dropping HNO_3 into Na_2WO_4	sccm	standard cubic centimeter per minute
		ppm	parts per million

1. Introduction

The sol-gel process is a facile fabrication technique where colloidal or gel can be prepared by mixing of liquid reactants which is first attempt in 1845 for the synthesis of hydrous silica[1]. To the best of our knowledge, sol-gel fabrication technique was only first demonstrated on the formation of tungsten oxide (WO_3) for its electrochromic property by Chemseddin on 1983[2]. Since then, intensive studies have been conducted for the fabrication of tungsten oxide by sol-gel method. There are three approaches to fabricate WO_3 by sol-gel method, which are acidification of sodium tungstate[3], dissolving tungsten powders in hydrogen peroxide[4] and reaction between tungsten oxy-chloride and isopropanol[5].

With only requirement of chemical reactants, sol-gel technique offers very simple and low synthesis cost to fabricate WO_3, which could also be synthesized in nanocrystalline structure by fine-tuning sol-gel parameters. Existing in a gel form or precipitation, sol-gel derived WO_3 can be coated on the large substrate by dip-coating[6], spray-coating[7] and screen-print[8] methods, where this is a huge advantage to manufacture a large and low cost electrochromic device which still remains as a challenge for commercialize purpose. Owing to this, most of the researches on the sol-gel synthesized tungsten oxide were done to improve the electrochromic properties of tungsten oxide. For the case of acidification of sodium tungstate, additive like H_2O_2 or oxalic acid[9] are usually added into the solution to stabilize the sol for better electrochromic properties. On the other side, relatively little study has been done to understand the fundamental details of the effects of sol-gel parameters (mixing and aging conditions such as flow rate of mixing, pH, time, and temperature) on the properties of tungsten oxide and other applications.

In this work, we demonstrate that the mixing sequences and aging durations of the reactants could significantly affect the properties of the as-grown WO_3 and also its gas sensor application.

2. Experimental procedure

2.1. Materials preparation

40 ml, 0.15 M Na_2WO_4 (BDH chemical Ltd Poole England) was added drop by drop from 25 ml burette into 15 ml 3 M nitric acid (HNO_3) under vigorous stirring. The sample was labeled as W-A. For the other experiment, all the experiment parameters were repeated and remained the same except that 3 M HNO_3 was added into 0.15 M Na_2WO_4. The sample was labeled as A-W. Samples were left aging at 25 °C for 30 days.

2.2. Materials and gas sensing characterization

Samples were characterized by field emission scanning electron microscope (FESEM, FEI Nova NanoSEM 450) and X-ray diffraction (HR-XRD, PANalytical X'Pert PRO εRD PWγ040) to study their morphological and structural properties. To examine the hydrogen sensing properties, the samples were screen-printed on 0.25x0.25 inches interdigitated gold electrodes from Synkera. Prior to the measurement, the devices were annealed at 400 °C for 2 h in ambient air. Hydrogen sensing measurements were conducted at room temperature in a conventional gas flow system with 2000 sccm flow rate of 1000 ppm concentration of hydrogen. Keithley 2400 source meter unit was employed for the current-voltage measurement.

3. Results and discussion

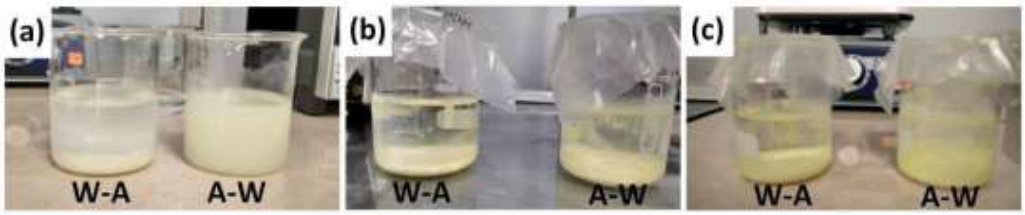

Fig. 1. Picture of W-A and A-W samples at (a) 10 min (b) 5 days (c) 30 days aging.

Fig. 1. clearly illustrates the difference of the mixing sequences of Na_2WO_4 and HNO_3 acid for different aging durations. For the W-A sample, precipitation could be observed during the mixing process, however for the A-W sample, the mixture appeared as yellowish solution during mixing process. These conditions remained the same after 10 min of experiment, as shown in Fig. 1(a). After 5 days of aging, precipitation could be detected for both of the samples. However, it is clear that the precipitations of A-W sample occupied higher volume and therefore it has less density since both mixtures have the same mixing volume of Na_2WO_4 and acid, as shown in Fig. 1(b). This implies that the structure formed in A-W condition has lower degree of polymerization, resulting in light and smaller polymerization chain. Same observation was detected as the sample further aging to 30 days, except that the precipitation with the milky yellowish color transformed into bright yellowish color, suggesting the formation of more tungsten oxide since it is more yellow in color. To further investigate the effect of aging duration on the morphological property, FESEM images were taken at different aging durations for the W-A sample, as shown in Fig. 2. After 1 day aging, no microstructure could be detected, as shown in Fig. 2(a) while after 5 aging day, FESEM image at Fig. 2(b) reveals that platelet structure could be seen which significantly improves in its uniformity after 30 days aging, as shown in Fig. 2(c) in low magnification scale.

Fig. 3. shows the FESEM top-view images of W-A and A-W samples after 30 days aging. It is evident that platelets structure of A-W sample is significant smaller in size compared to W-A sample where W-A sample has the platelets size of 1-1.θ ȝm while only β00-600 nm nanoplatelets were detected for A-W sample. This is an interesting result where much smaller platelets size could be obtained simply by changing the mixing sequence by adding acid into Na_2WO_4. As shown in fig. 4, XRD patterns reveal that both samples consist of crystalline $WO_3 \bullet \beta H_2O$, $WO_3 \bullet H_2O$ and WO_3. Both samples have similar XRD features, however, more intense and sharp peaks are observed for W-A sample, indicating better degree of crystallinity of W-A sample compared to A-W sample. There is no dominant orientation for A-W sample as three distinct peaks with similar peak intensities are observed on (020), **(**$1\bar{}$**11)** and (040) planes while for the W-A sample, (020) plane is the dominant orientation as it has ~4 times higher intensities to the other distinct peaks at (1$\bar{}$**11)**, (040) and (002).

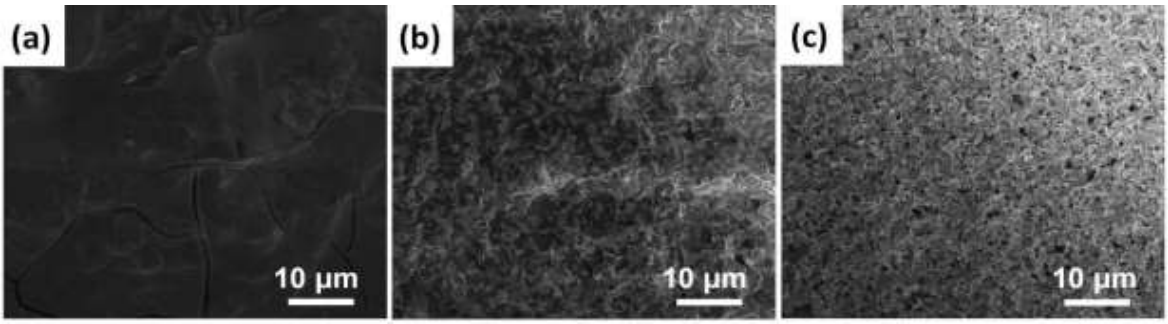

Fig. 2. FESEM top-view images of W-A sample after (a) 1 day, (b) 5 days and (c) 30 days aging in low magnification.

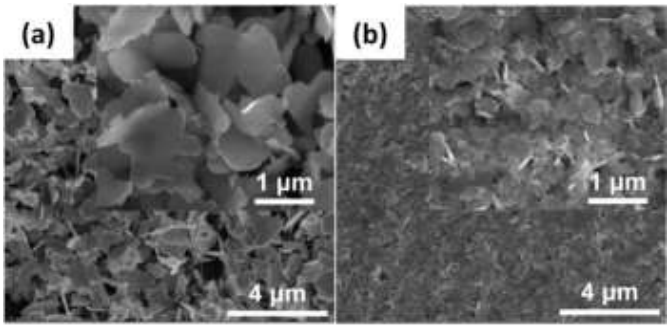

Fig. 3. FESEM top-view images of (a) W-A and (b) A-W samples after 30 days aging. The insets show magnified view of the samples.

Formation of different tungsten oxide structures of W-A and A-W samples could be ascribed to the different reaction conditions of WO_4^{2-} ions with the H^+ ions in the mixing process. It should be noted that for the W-A sample, Na_2WO_4 was dropped into HNO_3 acid where the WO_4^{2-} molecule will be surrounded by the excess of H^+ ions. The excess of H^+ ions will stimulate the rapid condensation polymerization, which will result in excess of ligands cross-linking to each other, forming extended oxides sheets of large platelets structure. This could explain the fast formation of dense precipitation and larger platelet size of the W-A sample. On the other hand, condensation polymerization process is very slow for the case of A-W condition as there are very limited amount of H^+ ions to trigger the condensation process since acid solution is dropped into Na_2WO_4 solution little by little in vigorous stirring condition. Consequently, the chances for the ligands to cross-link each other are less, resulting in a smaller size platelet structure.

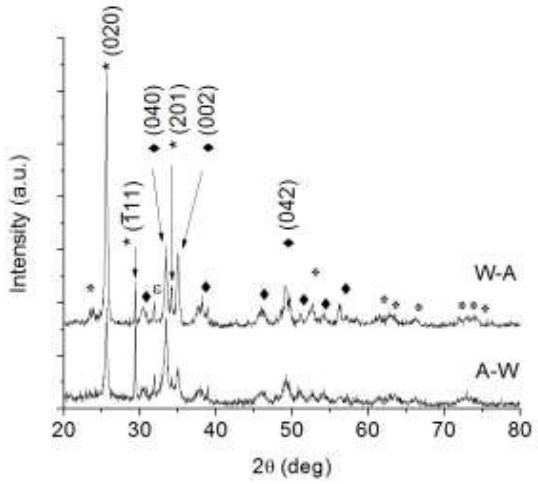

Fig. 4. XRD patterns of W-A and A-W samples after 30 days aging. Symbols _*', _♦' and _İ' indicate monoclinic WO_3•βH_2O, orthorhombic WO_3•H_2O and monoclinic WO_3.

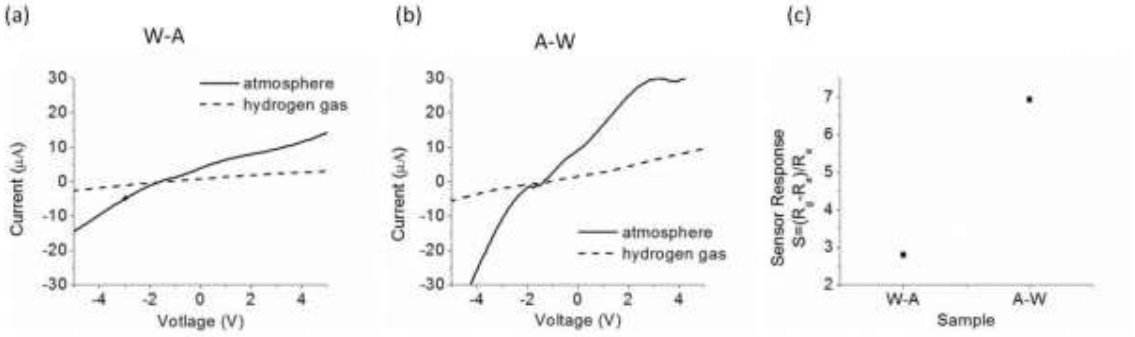

Fig. 5. Current-voltage characteristic curves of (a) W-A and (b) A-W samples at atmosphere and hydrogen gas condition. (c) Sensor response of the samples.

The hydrogen gas sensing properties of the samples were also examined at room temperature (25 °C) in 1000 ppm concentration of hydrogen, as shown in Fig. 5. Sensor response, S was defined as shown in equation 1 below, where R_g is defined as resistance of the device in hydrogen gas while R_a is defined as resistance of the device in ambient air.

$$S = \frac{R_g - R_a}{R_a} \quad (1)$$

Interestingly, both samples were able to exhibit hydrogen sensing properties even though at room temperature. However, it is evident that A-W device has a lower resistance at atmosphere condition and ~2.5 times higher sensor response compared to the W-A device. This observation is expected and this could be ascribed to the smaller platelet size of A-W device which has larger surface area to react with hydrogen gas compared to the microplatelet size of W-A device.

4. Conclusions

Effects of mixing sequence of sodium tungstate and nitric acid solution, as well as the aging duration on the formation of hydrated tungsten oxide by sol-gel method were examined in this work. For the tungsten oxide formed by dropping sodium tungstate into nitric acid (sample labeled as W-A), no structure could be detected after 1 day aging, while platelets structure of 1-1.θ 3m size were formed after 5 days aging, which further improves their uniformity after 30 days aging. By changing the dropping sequence to drop nitric acid into sodium tungstate (sample labeled as A-W), significantly smaller nanoplatelets of 200-600 nm were obtained. Both samples were crystalline hydrated tungsten oxide where W-A sample shows better degree of crystallinity. Room temperature hydrogen gas sensing property was detected by both samples where A-W sample with smaller nanoplatelets exhibit lower resistance in atmospheric condition and ~2.5 times higher sensor response to hydrogen gas compared to W-A sample.

Acknowledgements

The authors would like to thank Universiti Sains Malaysia for its financial support under USM-ERGS:203/PFIZIK/6730096 and USM-RU-PRGS:1001/PFIZIK/846079.

References

1. Ebelmen M. Comptes Rendus. *Acad Sci Fr* 1845;**21**:502.
2. Chemseddine A, Morineau R, Livage J. Electrochromism of colloidal tungsten oxide. *Solid State Ionics* 1983;**9**:357-62.
3. Zhangjun G, Tianyou Z, Bifen G, Xiaohai S, Yaobing W, Hongbing F, Ying M, Jiannian Y. Controllable assembly of WO_3 nanorods/nanowires into hierarchical nanostructures. *J Phys Chem B* 2006;**110**: 23829-36.
4. B. Munro, S. Kramer, P. Zapp, H. Krug. Characterization of electrochromic WO_3-layers prepared by sol-gel nanotechnology. *J Sol-Gel Sci Tech* 1998; **13**:673-8.
η. Judeinstein P, εorineau R, δivage J. Electrochemical degradation of WOγ•nH_2O thin films. *Solid Sate Ionics* 1992;**51**:239-47.
6. Cesar OA, Paulo RB, Luis OSB. Synthesis and electrochromic behavior of lithium-doped WO_3 films. *J Non-Cryst Solids* 2001;**290**:115-21.
7. Chiping L, Feng L, Ryan MR, Chaiwat E, Robert CT. The influence of sol-gel processing on the electrochromic properties of mesoporous WO3 films produced by ultrasonic spray deposition. *Sol Energy Mater Sol Cells* 2014;**121**:163-70.
8. Tetsuya K, Aya N, Masayoshi Y, Kengo S, Noboru Y. Highly sensitive NO_2 sensors using lamellar-structured WO_3 particles prepared by an acidification method. *Sens Act B* 2009;**135**:568-74.
9. Soliman HMA, Kashyout AB, Mohamed SEN, Abosehly AM. Effect of hydrogen peroxide and oxalic acid on electrochromic nanostructured tungsten oxide thin films. *Int J Electrochem Sci* 2012;**7**:258-71.